Effect of oxide inclusions on the solid state transformations in low-alloy steel fusion welds.

S. S. Babu†, S. A. David, and J. M. Vitek
Metals & Ceramic Division, Oak Ridge National Laboratory,

†The Pennsylvania State University, PA 16802, USA

Paper presented in 4th international conference on Trends in Welding Research, Gatlinburg, Tennessee, USA

DISCLAIMER

Abstract

Non-metallic inclusions are known to influence the properties of low alloy steel weld metal by altering the microstructure development. Isothermal transformation kinetics of austenite to acicular ferrite and allotriomorphic ferrite were measured in reheated low alloy steel weld deposits with similar weld compositions and austenite grain size but different inclusion characteristics. Accelerated kinetics of the transformation to acicular ferrite were observed in the weld metal containing coarser titanium-rich inclusions. The results are also discussed in relation to the predictions of inclusion model. The kinetics of the transformation to allotriomorphic ferrite were not influenced by a change in the inclusion characteristics, but, rather, by a change in austenite grain size. A theoretical analysis of austenite grain development during weld cooling is considered in this work. The austenite grain size was found to depend on the driving force for transformation from δ ferrite to austenite ($\Delta G^{\delta->\gamma}$) calculated from ThermoCalc™ software.

FUNDAMENTAL UNDERSTANDING OF VARIOUS physical processes that occur in fusion welding of steels is necessary to design new welding consumables and processes. The physical processes include evaporation of alloying elements in steel, dissolution of gases from arc atmosphere, oxide inclusion formation, solidification, solid state transformation and development of residual stresses (1–3). Various phase changes that occur as a function of weld cooling, in the weld metal region, are illustrated in a schematic diagram (Figure 1). The weld pool region is usually heated to temperatures as high as 2500 K. As the weld metal cools from this temperature, (I) in the temperature range 2300 to 1800 K, the dissolved oxygen and deoxidizing elements in liquid steel react to form complex oxide inclusions of 0.1–1μm size range; (II) in the temperature range 1800 to 1600 K, solidification of δ ferrite starts which envelops these oxide inclusions.

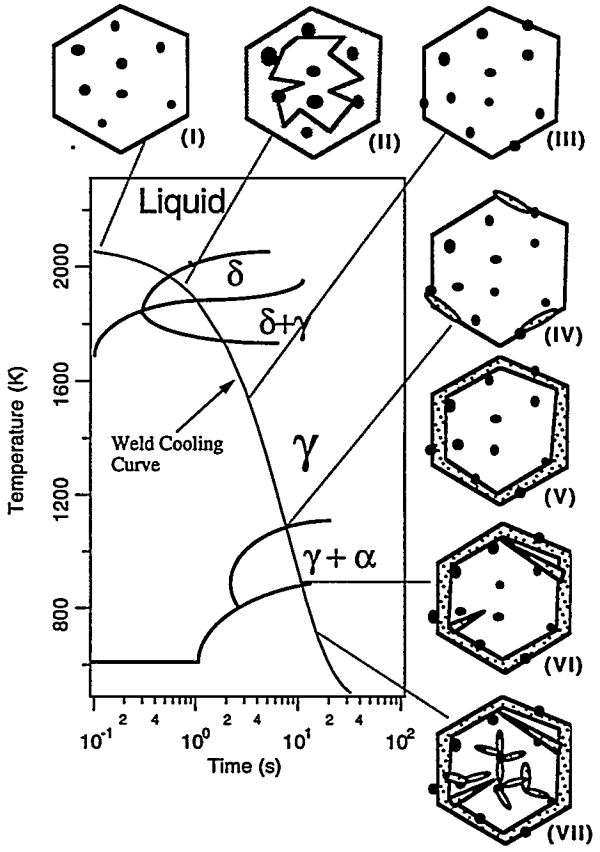

Figure 1 – (a) Schematic diagram of continuous cooling transformation diagram showing and the development of weld metal microstructure in the low alloy steels. (I) inclusion formation, (II) solidification of liquid to δ ferrite, (III) fully austenitic structure, (IV-V) nucleation and growth of allotriomorphic ferrite all along the austenite grain boundaries, (VI) Widmanstätten ferrite formation and (VII) acicular ferrite formation.

(III) Subsequently δ ferrite transforms to austenite; (IV–VII) finally in the temperature range 1100 to 500 K, the austenite transforms to different ferrite morphologies such as allotriomorphic ferrite, Widmanstätten ferrite and acicular ferrite (4). The optimum strength and toughness in steel welds are achieved by maximizing the amount of acicular ferrite. It is well known that the inclusions in steel welds promote the formation of acicular ferrite (4-6). Hence, there is a great need to understand the inclusion formation in liquid steel and its effect on transformation of austenite to various ferrite morphologies. In this paper the effect of inclusions on transformation kinetics of austenite to allotriomorphic and acicular ferrite is discussed. Moreover, the development of austenite grains from δ ferrite is related to the thermodynamics of transformation from δ ferrite to austenite.

Experimental

Since the inclusion characteristics are known to influence the microstructure development in steel welds, it is desirable to study only the influence of inclusion characteristics on the transformation kinetics of allotriomorphic ferrite, Widmanstätten ferrite, and acicular ferrite. In this work the transformation kinetics of allotriomorphic ferrite and acicular ferrite were measured for two different inclusion characteristics. Two submerged arc welds with two different inclusion characteristics were produced by varying the weld metal composition. The weld metal compositions and welding process conditions are given in Table I. The inclusion characteristics were analyzed in a Philips CM-12 transmission electron microscope by the extraction replica technique. The isothermal and continuous cooling heat treatments were performed in a Gleeble™ thermomechanical simulator and transformation kinetics were obtained by dilatometric technique. The weld metal hardenability and the prior austenite grain size were designed to be similar in both welds SW1A and SW2A.

Table I. Weld metal compositions of submerged arc welds used in this investigation. Welding parameters for both welds are: welding voltage 29 V, welding current 580 A, and welding speed 9×10^{-3} ms^{-1}.

Welds	C	Si	Mn	Ti	Al	O
SW1A	0.10	0.81	1.61	0.018	0.015	0.084
SW2A	0.10	0.35	1.67	0.003	0.014	0.029

Theoretical time–temperature transformation diagram calculations (7) indicated the change in silicon levels between welds SW1A and SW2A may not influence the transformation kinetics of allotriomorphic ferrite and acicular ferrite. The austenite grain size was maintained at ~70 μm by austenitizing the samples at 1473 K for 0.6 ks. The continuous cooling transformation kinetics were measured in the 1 to 50 K s^{-1} range. The details of the isothermal heat treatments are given in Table II. Although the results of isothermal transformation kinetics of allotriomorphic ferrite and acicular ferrite are published elsewhere (8), the results are discussed again with reference to predictions of inclusion model. The kinetic measurements were performed by dilatometric techniques and the details of the procedure are published elsewhere (8). The measured isothermal kinetics were then compared with the theoretical transformation kinetic equations.

Table II. Tabulation of heat treatments and measured austenite grain size.

ID	Austenitization treatment	Austenite grain size, μm		Isothermal transformation
		SW1A	SW2A	
HT1	1473 K, 0.6 ks	71 ± 4	69 ± 3	953 K, 1.2 ks
HT2	1473 K, 0.6 ks	71 ± 4	69 ± 3	843 K, 0.6 ks

Results and Discussion

The experimentally measured inclusion characteristics are presented in Table. III. As expected, the change in weld metal composition lead to a change in the inclusion characteristics. Since the experimental inclusion characteristics of SW1A and SW2A (Table III) are different, a change in the transformation kinetics of ferrite from austenite is also expected. The comparison of CCT behavior is shown in Figure 2. The plots show that the transformation characteristics are almost identical for all the cooling rates in both the weld samples. Although, this result suggests that there is no change in the transformation kinetics due to a change in the inclusion characteristics, it is difficult to differentiate the effect of inclusions on allotriomorphic ferrite and acicular ferrite kinetics. Therefore, further isothermal transformation kinetic studies were performed.

Table III. Experimental inclusion characteristics of welds SW1A and SW2A.

Weld No.	Inclusion Size, μm	Num. Density x10^{16} m^{-3}	Inclusion Composition, wt.%			
			Al	Ti	Si	Mn
SW1A	0.84	3.0	13.0	11.0	26.0	48.0
SW2A	0.53	3.6	29.0	3.0	25.0	43.0

Allotriomorphic ferrite transformation kinetics: To study the effect of inclusions, one needs to study the measured transformation kinetics in terms of theoretical kinetic equations in the early stages of allotriomorphic ferrite growth. The transformation kinetics of allotriomorphic ferrite are controlled by nucleation and growth mechanisms. Bhadeshia *et al.* (9) presented a model based on nucleation and growth. The allotriomorphic ferrite, before site saturation, is modeled as disc with the faces parallel to the austenite grain boundary plane and is assumed to grow in a radial direction. The

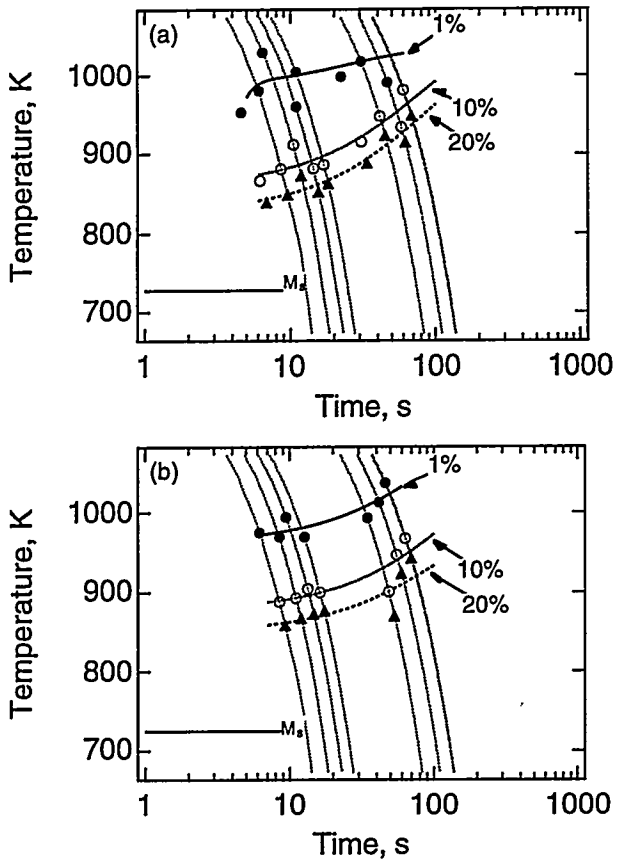

Fig. 2 – Comparison of measured continuous cooling transformation characteristics from welds (a) SW1A and (b) SW2A. The austenitization condition was 0.6 ks at 1473 K. The austenite grain sizes in both the samples were similar at ~70 μm. The measured cooling curves (dotted lines) are also shown. The experimental data points and fitted lines for 1%, 10% and 20% transformation are shown in the plot.

final expression relating the extent of reaction ζ, defined as the ratio of measured volume fraction to equilibrium volume fraction, the parabolic thickening rate (α_1), the grain boundary nucleation rate per unit area (I_B), and the reaction time (t) is given as

$$-\ln\{1-\zeta\} = f\{\eta\alpha_1, I_B, t\} \times 2(S_V/\phi)\alpha_1\sqrt{t} \qquad (1)$$

where η is the aspect ratio of the discs of allotriomorphic ferrite, S_V is the austenite grain boundary area per unit volume and ϕ is the equilibrium volume fraction expected at a particular temperature and

$$f\{\eta\alpha_1, I_B, t\} = \int_0^1 [1-\exp\left\{\frac{-\pi I_B(\eta\alpha_1)^2 t^2(1-\theta^4)}{2}\right\}]d\theta \qquad (2)$$

where $\theta = y/(\alpha_1 t^{0.5})$ and y is the distance from the grain boundary plane. The term $f\{\eta\alpha_1, I_B, t\}$ approaches unity as the site saturation occurs, after which, the kinetics are controlled by the parabolic thickening rate α_1 and S_V, until the overlap of diffusion profiles occurs (soft impingement). The equation 1 cannot be applied after soft impingement (9). It is known that the austenite grain boundaries are energetically preferred sites for the allotriomorphic ferrite nucleation compared to the inclusions within the austenite grain. However, the inclusions that lie along a austenite grain boundary plane may modify the inherent nucleation potency of the boundary. As a result, the kinetics of allotriomorphic ferrite may vary with inclusion characteristics, as suggested in reference (5). The allotriomorphic ferrite transformation kinetics measured in the steel welds with two different inclusion characteristics (similar austenite grain size) are analyzed with equation 1.

The measured volume fraction of allotriomorphic ferrite was converted into extent of reaction, ζ. The $-ln\{1-\zeta\}$ term of equation 1 can be plotted as a function of the square root of transformation time, $t^{0.5}$. According to equation 1, this term is expected to increase non-linearly until nucleation site saturation occurs, where $f\{\eta\alpha_1, I_B, t\} = 1$. Only during this initial stage, the inclusions may influence the nucleation of allotriomorphic ferrite. Hence, for a similar composition and austenite grain size (or S_V) the time for site saturation, τ, is expected to be different if the inclusions have an influence on I_B. The plots of $-ln\{1-\zeta\}$ terms against $t^{0.5}$, for SW1A and SW2A in HT1 treatment, are shown in Figure 3. The time for site saturation (τ) is marked in the plots. The plots show negligible difference in the time for site saturation. According to equation 1, after the site saturation, the $-ln\{1-\zeta\}$ term will vary linearly with a slope of $(2S_V\alpha_1)/\phi$. The slopes after site saturation are almost identical indicating that both alloys have the same values of $(2S_V\alpha_1)/\phi$.

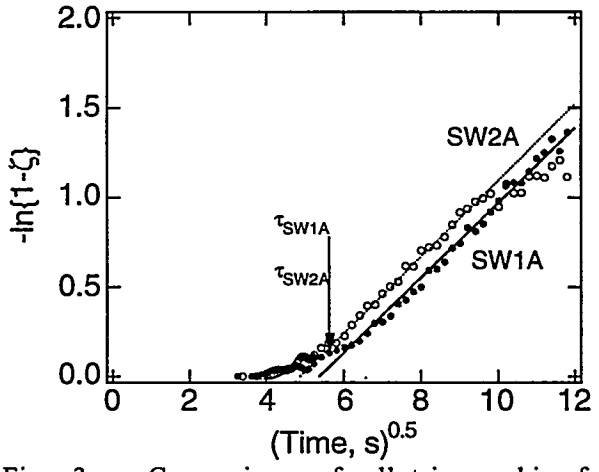

Fig. 3 – Comparison of allotriomorphic ferrite transformation kinetics at 953 K in welds SW1A and SW2A. The prior austenite grain sizes are similar for both the welds. The dotted and solid lines show the slope of the curves during parabolic growth region. The slope values were found to be 0.20 for SW1A and 0.21 for SW2A.

This result indicates that the transformation kinetics of SW1A and SW2A are approximately the same and there is no significant effect of the inclusion characteristics on the allotriomorphic ferrite transformation kinetics. However, in real welding conditions, the inclusions may indirectly influence the allotriomorphic ferrite kinetics. For example, as observed by Fleck *et al.*

(10) for identical weld compositions, increase in the inclusion volume fraction reduces the austenite grain size. The reduction in the austenite grain size leads to an increase in the value of S_V and the transformation kinetics are enhanced. Previous work (8) has clearly shown that the isothermal allotriomorphic ferrite transformation kinetics are quite sensitive to the austenite grain size.

Acicular ferrite transformation kinetics: It is known that inclusions rich in titanium promote the formation of acicular ferrite. The experimental inclusion characteristics presented in Table III show that the inclusions in weld SW1A are coarser and richer in titanium than the inclusions in weld SW2A. Therefore a resulting change in the transformation kinetics of acicular ferrite is expected. The measured kinetic plot of acicular ferrite (in SW1A and SW2A during HT2 heat treatment) is shown in Figure 4. The measured volume fraction of acicular ferrite at 843K is converted into the extent of acicular ferrite transformation, ζ. The extent of acicular ferrite transformation is given by the ratio of the measured volume fraction to the expected volume fraction of acicular ferrite. The value of expected volume fraction of acicular ferrite is given by the T_0 boundary at 843 K (i.e., where the austenite and ferrite with similar composition have equal free energy) with a ferrite strain energy of 400 J mole^{-1} (11). The acicular ferrite kinetic results showed that the transformation kinetics are indeed accelerated in weld SW1A compared to those in SW2A.

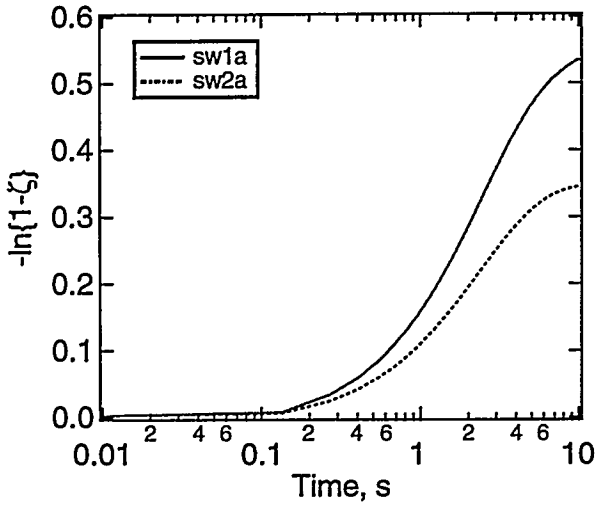

Fig. 4 – Comparison of acicular ferrite transformation kinetics at 843 K in welds SW1A and SW2A. The prior austenite grain sizes are similar for both the welds.

According to the above observation, the acicular ferrite microstructures of SW1A and SW2A are expected to be different after the HT2 heat treatment. However, the microstructures (Fig. 5) in the samples showed no apparent difference. This is because the microstructure after this heat treatment could not be quenched to the room temperature. The residual austenite in both SW1A and SW2A transformed to acicular ferrite during cooling from 843K to room temperature and the microstructure difference at 843K was lost. Hence, the difference in transformation kinetics to acicular ferrite due to a change in inclusion characteristics can not be discerned from the final microstructure in these welds. However, the direct kinetic measurement by dilatometry, at a particular temperature, indicated a difference in kinetics does exist.

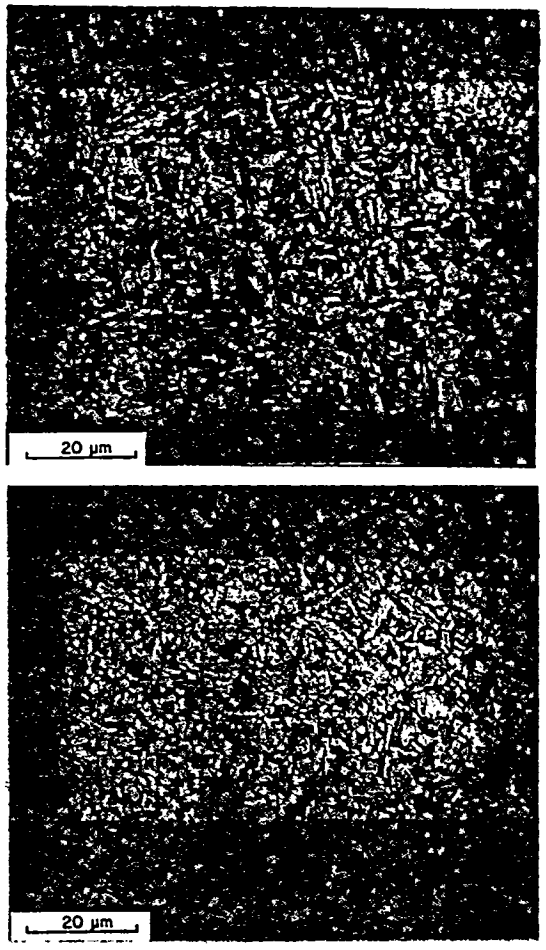

Fig. 5 – Comparison of final microstructure of (a) SW1A and (b) SW2A after HT2 heat treatment.

The accelerated transformation kinetics of austenite to acicular ferrite due to a change in the inclusion characteristics may be related to heterogeneous nucleation of ferrite on inclusions. The heterogeneous nucleation of ferrite on inclusions may be related to the following mechanisms: (a) low lattice misfit between the inclusion and ferrite, (b) inclusions acting as high energy inert substrates, (c) chemical inhomogeneity around the inclusions, and (d) localized thermal strains around inclusions. It is known that Ti–rich (Ti_xO_y type) and Galaxite type compounds on the inclusion surface may promote the formation of acicular ferrite (6). A comprehensive model (12,13) for inclusion formation was used to calculate the inclusion characteristics for SW1A and SW2A wekds. The inclusion model is capable of calculating the oxidation sequence during deoxidation reactions in steel weld metal. The oxidation sequence calculated by the inclusion model is given in Table IV.

The calculations show that the proportion of $MnOAl_2O_3$ (Galaxite) is more in SW1A than that of SW2A. However, in both welds the formation of Ti_xO_y type oxide is predicted. Therefore, the results from inclusion model suggest that the presence of Ti_xO_y type oxide may not be as important as Galaxite in determining the acicular ferrite transformation kinetics in the welds SW1A and SW2A. However, the existence of $MnOAl_2O_3$ on the surface of inclusions has to be confirmed by electron diffraction analysis in future work. Moreover, the above inclusion formation model has to be coupled with the theoretical overall transformation kinetic equations of acicular ferrite to estimate transformation kinetics as a function of weld metal composition, inclusion characteristics and weld metal cooling rate.

Table IV – Oxidation sequence calculated by the inclusion model for welds SW1A and SW2A (Table 1). The table indicates the type of oxides that form as a function of temperature, as the welds cool from 2300K.

SW1A Weld		SW2A Weld	
Temperature, K	Oxide	Temperature, K	Oxide
2134	Al_2O_3	2073	Al_2O_3
2109	Ti_3O_5	2012	$MnOAl_2O_3$
2094	SiO_2	1938	Ti_3O_5
2087	$MnOAl_2O_3$	1889	SiO_2
2080	$MnOAl_2O_3$	1851	Ti_2O_3
2038	SiO_2	1828	SiO_2
2033	$MnOAl_2O_3$		
2025	$MnOAl_2O_3$		
2015	$MnOAl_2O_3$		
2004	$MnOAl_2O_3$		
1990	$MnOAl_2O_3$		
1972	$MnOAl_2O_3$		
1946	$MnOAl_2O_3$		
1940	SiO_2		
1836	$MnOAl_2O_3$		

Weld metal austenite grain size: Since the austenite grain size affects the transformation kinetics to a greater extent, it is important to understand the austenite grain development in low alloy steel welds. The austenite grain development during weld cooling is related to two reactions i.e., (a) transformation of δ ferrite to austenite during cooling by nucleation and growth at δ ferrite grain boundaries, and (b) austenite grain growth after the completion of the δ ferrite to austenite transformation during weld cooling. In this work, a theoretical analysis was performed to relate the driving force for transformation of δ ferrite to austenite ($\Delta G^{\delta->\gamma}$) to the experimental austenite grain size measured by Evans (14). Evans has measured the prior austenite grain size as a function weld metal composition for the same welding heat input. The driving force for transformation of δ ferrite to austenite ($\Delta G^{\delta->\gamma}$) for the same compositions was calculated from ThermoCalc™ (15) software. In this calculation, the following assumptions are made for simplicity:

(a) Differential thermal analysis (DTA) performed on low alloy steel weld metal compositions (16), similar to that of Evans(14) weld metal compositions, illustrated that solidification to δ ferrite and transformation to austenite completed at 1661 K as the weld metal cooled at 1 Ks^{-1} from the liquidus temperature. It is important to note that the weld metal cooling rates are higher than 1 Ks^{-1} (> 50 Ks^{-1}). Since there are no experimental data on the transformation start temperature of austenite from δ ferrite, in this analysis, the transformation from ferrite to austenite is assumed to occur isothermally at a particular undercooling and this temperature is taken as 1673 K. However, in future work the method described below can be easily modified for continuous cooling conditions;
(b) The austenite grain size is assumed to be inversely proportional to nucleation rate of austenite at the δ ferrite grain boundary, where the nucleation rate is a function of $\Delta G^{\delta->\gamma}$ as shown below.

$$Grain\ Size = 1/(nucleation\ rate)^A \quad (3)$$

where A is the constant exponent and the nucleation rate is given by the expression

$$nucleation\ rate = B + C\ exp\{-D/(\Delta G^{\delta->\gamma})^2\} \quad (4)$$

where B and C are constants.
(c) In this analysis since the austenite nucleation events occur at δ ferrite grain boundary during rapid weld cooling conditions, the alloying element partitioning during nucleation is not considered. The compositions of austenite and ferrite are assumed to be the same.

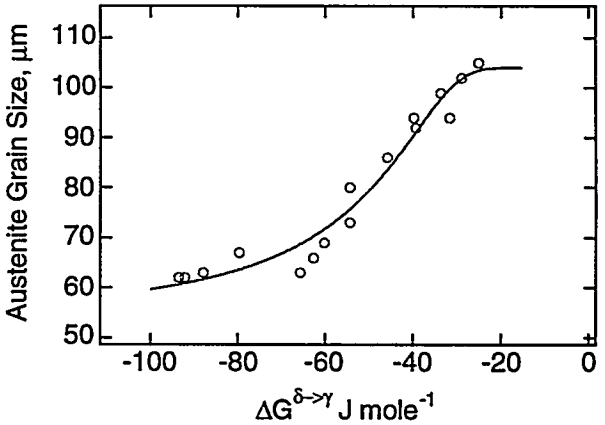

Fig. 6 –The variation of austenite grain size with driving force for transformation of δ ferrite to austenite ($\Delta G^{\delta->\gamma}$). The dark line is the fitted line with a relation given by the equations 3 and 4. Experimental data (open circles) are from reference 14.

The experimental austenite grain size (in the units of meters) and the calculated $\Delta G^{\delta->\gamma}$ (in the units of J $mole^{-1}$) are fitted to equations 3 and 4. The fitted constants are as follows: A=0.48974: B=1.356x10^8; C=4.0869x10^8; and D=3525.4. The correlation between the predicted and

experimental data is shown as a function of $\Delta G^{\delta->\gamma}$ in Figure 6. This result shows that austenite grain size estimation for a constant heat input can be made with a knowledge of $\Delta G^{\delta->\gamma}$ from thermodynamic calculations and demonstrates the sensitivity of the austenite grain development to the driving force for transformation of δ ferrite to austenite. However, this simple calculation has to be modified to the continuous cooling conditions and to a change in the weld heat input. Unfortunately, there is no detailed analysis of the austenite grain size variation with regard to a change in inclusion characteristics. Further work is necessary in this area.

General Discussions: The work presented in this paper has shown that the microstructure development in low alloy steel weld depends are sensitive to inclusion characteristics, austenite grain size, and weld metal composition. However, the discussions in the above paper have not addressed (a) the effect of inclusions on austenite grain development, (b) the mechanism by which the inclusions nucleate acicular ferrite, and (c) the interaction of the external and internal mechanical forces that develop in steel weldments on microstructure development. Further work is underway to study the mechanism of inclusion nucleation potency by applying elastic stresses during acicular ferrite transformation. Moreover, as pointed out by Kirkaldy (17) the microstructure development and mechanical forces interact with each other during steel processing and service conditions. For example, it is known that acicular ferrite transformation behavior is quite sensitive to external forces. In the work by Babu and Bhadeshia (18), the acicular ferrite microstructure evolution in a steel weld was found to comply with an externally applied elastic stress and the samples exhibited transformation induced plasticity during isothermal transformation. This phenomenon will have due influence on the residual stress development in steel welds. Therefore, future modeling work on the development of microstructure in low alloy steel welds has to consider the effect of external and internal stress conditions.

Summary and Conclusions

The transformation kinetics of allotriomorphic ferrite and acicular ferrite were measured in two steel welds with two different inclusion characteristics but with similar austenite grain size. The allotriomorphic ferrite transformation kinetics were found to be independent of inclusion characteristics. Acicular ferrite transformation kinetics were found to be dependent on the inclusion characteristics. The accelerated acicular ferrite transformation may be related to the presence of Galaxite oxides in the inclusions. The austenite grain size development in steel welds is related to the driving force for transformation from δ ferrite to austenite.

Acknowledgments

This research sponsored by the Division of Materials Sciences, U. S. Department of Energy, under contract DE-AC05-84OR21400 with Lockheed Martin Energy Systems, Inc. The authors thank Dr. L.–E. Svensson of ESAB Sweden and Mr. S. Ferree of Alloy Rods Inc., Hanover, PA, USA for supplying the welds used in the present investigation. The authors also thank Dr. A. N. Gubbi of ORNL for reviewing the paper.

References

1. David, S. A., and DebRoy, T., Science, 257, 497-502, (1994).

2. David, S. A., DebRoy, T. and Vitek, J. M., MRS Bulletin, XIX, 29-35, (1994).

3. DebRoy, T., and David, S. A., Reviews of Modern Physics, 67, 85–112.

4. Bhadeshia, H. K. D. H., and Svensson, L.–E., in Mathematical modeling of weld phenomena, edited by H. Cerjak and K. E. Easterling, The Institute of Materials, London, UK., 1993, p. 109-178.

5. Abson, D. J., and Pargeter, R. J., Int. Met. Reviews, 31, 141-194, (1986).

5. Grong, Ø. and Matlock, D. K., Int. Met. Reviews, 31, 27-48, (1986).

6. H. K. D. H. Bhadeshia, Bainite in Steels, 1992, p. 243-282. The Institute of Materials, London, U. K.

7. Bhadeshia, H. K. D. H., Metal Science, 16, 159–165, (1982).

8. Babu, S. S., David, S. A., Vitek, J. M., and DebRoy, T., in Solid->Solid phase transformations, edited by W. C. Johnson, J. M. Howe, D. E. Laughlin and W. A. Soffa, The Metallurgical Society of AIME, Warrendale, PA, USA, 1994, p. 213–218.

9. Bhadeshia, H. K. D. H., Svensson, L.–E., and Gretoft, B., in Proc. International Conference on Welding Metallurgy of Structural Steels, Edited by J. Y. Koo The Metallurgical Society of AIME, Warrendale, PA, USA, 1987, p. 517-530.

10. Fleck, N. A., Grong, Ø., Edwards, G. R., and Matlock, D. K., Welding Journal, 65, 113s-121s, (1986).

11. Bhadeshia, H. K. D. H., Acta. Metall., 29, 1117-1130, (1981).

12. Babu, S. S., David, S. A., Vitek, J. M., Mundra, K., and DebRoy, T., Materials Science and Technology,

13. Babu et al in this conference proceeding

14. Evans, G. M., Welding Journal, 62,313s-320s, (1983).

15. Sundman, B., Jansson, B., and Andersson, J. –O., Calphad, 9, 153-190, (1985).

16. Babu, S. S., David, S. A., and Vitek, J. M. unpublished research, Oak Ridge National Laboratory, 1995.

17. Kirkaldy, J. S., Scandinavian Journal of Metallurgy, 20, 55-61, 1991.

18. Babu, S. S., and Bhadeshia, H. K. D. H., Materials Science and Engineering, A156, 1-9, (1992).